

## Local characterization of phases and phase transitions in $\text{BaZrF}_6$

This article has been downloaded from IOPscience. Please scroll down to see the full text article.

1998 J. Phys.: Condens. Matter 10 2893

(<http://iopscience.iop.org/0953-8984/10/13/008>)

View [the table of contents for this issue](#), or go to the [journal homepage](#) for more

Download details:

IP Address: 171.66.16.209

The article was downloaded on 14/05/2010 at 12:49

Please note that [terms and conditions apply](#).

## Local characterization of phases and phase transitions in BaZrF<sub>6</sub>

M A Taylor†§, J A Martínez†||, A López García†§ and M Dejneka‡

† Departamento de Física, Facultad de Ciencias Exactas, Universidad Nacional de La Plata, CC 67, 1900 La Plata, Argentina

‡ Corning Incorporated, SP-FR-5, Sullivan Park, Corning, NY 14831, USA

Received 20 August 1997, in final form 28 November 1997

**Abstract.** The hyperfine quadrupole interaction of BaZrF<sub>6</sub> was determined in the room-temperature to 720 °C range. The study of the thermal behaviour of the hyperfine parameters identified an extended phase transition from  $\alpha$ -BaZrF<sub>6</sub> to  $\beta$ -BaZrF<sub>6</sub> and the existence of a distorted low-temperature  $\beta$ -phase.

### 1. Introduction

Zirconium fluoride based glasses have been extensively studied in recent years ([1, 2] and references therein). The thermal and chemical stability of this kind of glass are of great importance from the technological point of view, mainly because of its uses as optical fibres. The ones so extensively examined are the BaF<sub>2</sub>-ZrF<sub>4</sub> glasses as a prototype of fluorozirconate glasses ([3, 4] and references therein). This kind of glass has a tendency to devitrify during preparation and fabrication and in order to achieve good optical properties the formation of crystallites must be prevented.

The phase diagram of the BaF<sub>2</sub>-ZrF<sub>4</sub> system exhibits seven stoichiometric phases ( $\alpha$ - and  $\beta$ -BaZrF<sub>6</sub>,  $\alpha$ - and  $\beta$ -BaZr<sub>2</sub>F<sub>10</sub>, Ba<sub>3</sub>ZrF<sub>10</sub>, Ba<sub>4</sub>Zr<sub>2</sub>F<sub>16</sub> and Ba<sub>0.65</sub>Zr<sub>0.35</sub>F<sub>2.70</sub>) and two nonstoichiometric phases [5]. Nevertheless, within the range of compositions where glasses are obtained, only two crystalline compounds are expected to be formed: BaZrF<sub>6</sub> and BaZr<sub>2</sub>F<sub>10</sub>, the first one being the most probable while a glass crystallizes [6].

The BaZrF<sub>6</sub> crystallizes at room temperature in the monoclinic space group  $P2_1/c$ . The structure is built up of single [Zr<sub>2</sub>F<sub>12</sub>]<sup>4-</sup> complex anions resulting from the association of two monocapped trigonal prisms sharing one edge, linked by Ba<sup>2+</sup> cations [7]. By means of DTA experiments, Laval *et al* have established that BaZrF<sub>6</sub> experiences a reversible  $\alpha \leftrightarrow \beta$  phase transition at  $544 \pm 5$  °C. The  $\beta$ -BaZrF<sub>6</sub> phase is orthorhombic, with space group  $Abm2$  [8].

A specially suited technique to deal with the microscopic study of zirconium based substances is the time differential perturbed angular correlation (PAC) technique using <sup>181</sup>Hf (<sup>181</sup>Ta) as a hyperfine probe. In order to perform a study of the stability of the ZrF<sub>4</sub>/BaF<sub>2</sub> based glasses, it is important to know in advance the hyperfine characteristic of the crystalline phases involved during crystallization processes. With this purpose, the

§ Member of Carrera del Investigador Científico CONICET, Argentina.

|| Member of Carrera del Investigador Científico CICPBA, Argentina.

PAC technique was used to determine the quadrupole interaction between the  $^{181}\text{Ta}$  probe nuclei and their surrounding in  $\text{BaZrF}_6$  and its thermal dependence in the range from room temperature (RT) to  $720^\circ\text{C}$ .

## 2. Experiment

The PAC technique determines the hyperfine interaction between a radioactive nucleus, decaying through a two-step cascade, and its surroundings by measuring the time dependence of the angular distribution of the second nuclear emission (within the order of the mean life of the intermediate state of the cascade) relative to the direction of the first one. In the case of a static quadrupole interaction, a perturbation of the angular distribution arises from the electric field gradient (EFG) created by the nearby charge distribution, acting on the quadrupole moment ( $Q$ ) of the intermediate nuclear level of the cascade. This perturbation is described by the attenuation factor  $G_{22}(t)$  which, for a  $\gamma$ - $\gamma$  cascade in polycrystalline samples, takes the form:

$$G_{22}(t) = \sigma_{20} + \sum_{i=1}^3 \sigma_{2i} \cos(\omega_i t) e^{(-\delta\bar{\omega}_i t)}$$

where  $\sigma_{2i}$  and  $\omega_i$  are known functions of the quadrupole frequency  $\omega_Q = eQV_{zz}/4I(2I-1)\hbar$  ( $I$  being the nuclear spin of the intermediate level) and of the asymmetry parameter of the electric field gradient  $\eta = (V_{xx} - V_{yy})/V_{zz}$ . The frequency distribution width  $\delta$  describes a Lorentzian frequency distribution around  $\omega_i$  due to lattice imperfections and/or impurities. The standard interpretation of the parameters involved in the attenuation factor can be summarized as follows: the frequencies  $\omega_i$  are associated with the transition between the sub-levels of the intermediate state as it is split by the electric field gradient; the asymmetry parameter characterizes the symmetry of the electric field gradient acting on the probe and varies from 0 to 1 (symmetric EFG and fully asymmetric EFG respectively) if the EFG's components are chosen such that  $|V_{zz}| \geq |V_{yy}| \geq |V_{xx}|$ . The coefficients  $\sigma_{2i}$  are related to the orientation of the EFG components in the frame of the detectors. Different values for the  $\sigma_{2i}$  coefficients than those expected for polycrystalline samples clearly indicate preferential orientation of the micro-crystals which constitutes the sample. Details of the technique and physical background are given elsewhere [9].

To consider inequivalent chemical environments, a linear combination of attenuation factors  $G_{22}(t) = \sum f_i G_{22i}(t)$  is used. In this case the coefficients  $f_i$  are interpreted as the relative fractions of the probes experiencing each environment. A non-linear least-squares fit procedure of the attenuation factor to the experimental data allows us to determine  $f$ ,  $\omega_Q$ ,  $\eta$  and  $\delta$  associated with each non-equivalent probe site.

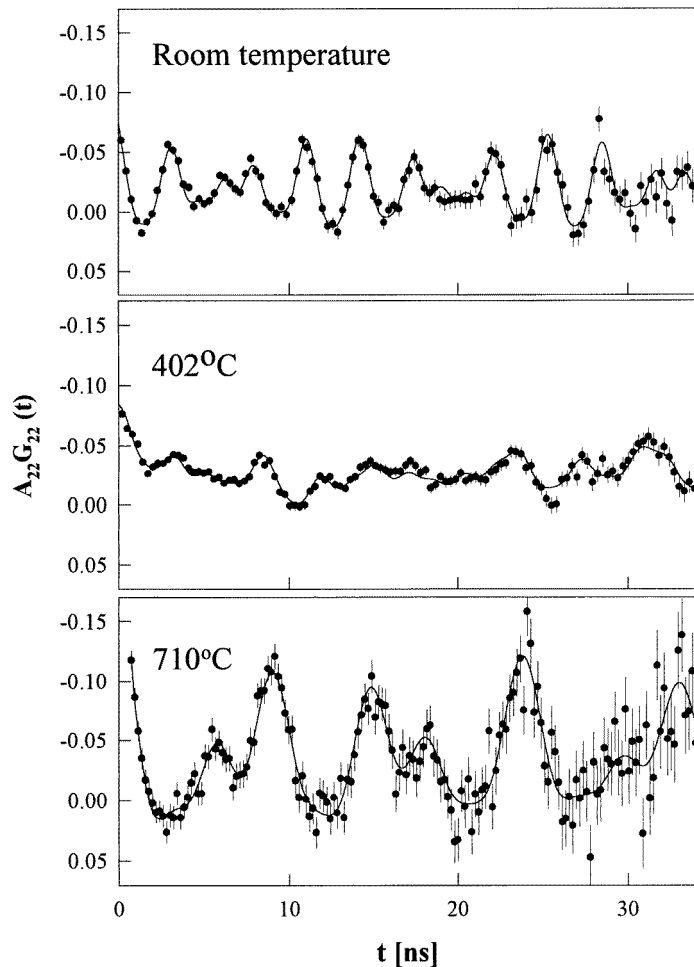
The  $\text{BaZrF}_6$  sample was prepared by weighing and mixing in a vitreous carbon crucible 50  $\text{BaF}_2$ , 49  $\text{ZrF}_4$  and 1  $\text{HfF}_4$  (in mol%). The mixture was heated to  $900^\circ\text{C}$  and treated with a 10:1  $\text{N}_2:\text{SF}_6$  reactive atmosphere for 60 minutes to remove residual water and oxide contamination. The melt was allowed to slowly cool to form the crystals.

The x-ray powder diffraction pattern was used to identify the phases present in the sample. The as-prepared sample corresponds to  $\alpha$ - $\text{BaZrF}_6$ . The compound was encapsulated in argon at atmospheric pressure in  $0.5\text{ cm}^3$  sealed quartz tubes. The activity of  $^{181}\text{Hf}$ , giving rise to the 133–482 keV  $\gamma$ - $\gamma$  cascade of  $^{181}\text{Ta}$  used in this work as a PAC probe, was obtained by thermal neutron irradiation of the sample in a flux of  $10^{13}\text{ cm}^{-2}\text{ s}^{-1}$ .

Measurements were performed using a conventional two-CsF-detector experimental set-up with a time resolution of  $2\tau = 0.8\text{ ns}$  at Ta energies, supplied with an electric furnace that allowed heating of the sample *in situ* within  $\pm 1^\circ\text{C}$ .

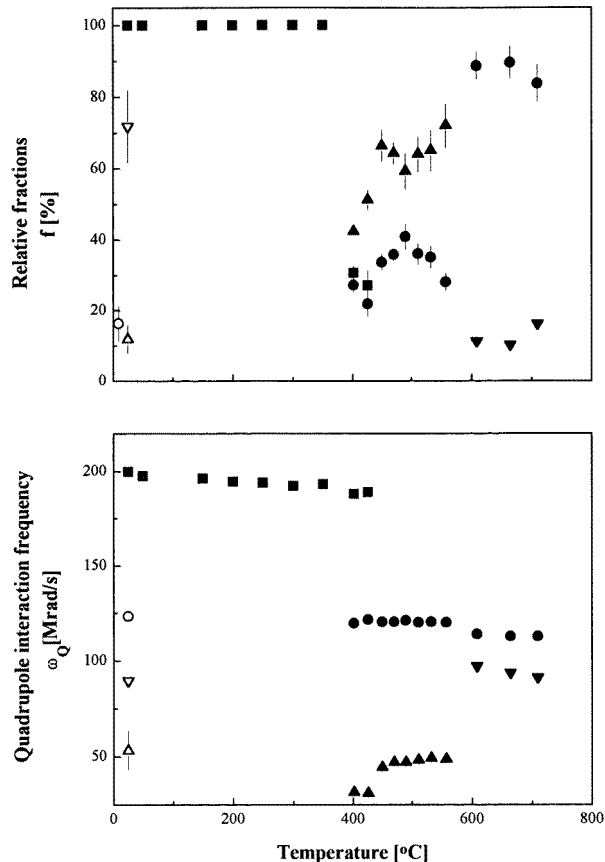
### 3. Results and discussion

Figure 1 shows typical PAC spectra obtained during the experiments. Data were fitted using static quadrupole interactions. Figure 2 shows the behaviour of the hyperfine parameters in the whole thermal range.



**Figure 1.** PAC spectra at temperatures where the most significant changes occur. Full lines are the fitted curves to the data.

The thermal evolution of the hyperfine interactions observed will be summarized as follows: below 400 °C, a unique well defined static quadrupole interaction with hyperfine parameters of about  $\omega_Q = 195 \text{ Mrad s}^{-1}$  and  $\eta = 0.74$ , was enough to reproduce the experimental data. In the range between 400 and 560 °C, the former interaction vanishes in a thermal interval of about 50 °C. Two new quadrupole interactions were needed to describe the data over all this range: a well behaved quadrupole interaction of about  $\omega_Q = 119 \text{ Mrad s}^{-1}$ ,  $\eta = 0.37$ ,  $\delta \cong 0\%$  (circles in figure 2) and another quadrupole interaction of about  $\omega_Q = 48 \text{ Mrad s}^{-1}$ ,  $\eta = 0$  having a rather varying distribution (up triangles in figure 2). Above 560 °C, the low-frequency interaction was replaced



**Figure 2.** Thermal evolution of the hyperfine parameters and relative fractions drawn from the fitting procedure. Squares corresponds to  $\alpha$ -BaZrF<sub>6</sub>, circles (open and full) correspond to  $\beta$ -BaZrF<sub>6</sub>, down triangles (open and full) correspond to distorted  $\beta$ -BaZrF<sub>6</sub>, up triangles (open and full) correspond to the intermediate state. Open symbols represent obtained at room temperature after measuring at 560 °C.

by a new one (down triangles in figure 2) whose hyperfine parameters were around  $\omega_Q = 100 \text{ Mrad s}^{-1}$ ,  $\eta = 0.15$ ,  $\delta < 5\%$  and whose relative fraction remained less than 20%.

In order to interpret the evolution of PAC results, RT x-ray analysis in a sample heated at 400 °C and then at 600 °C for one day (temperatures at which the most significant PAC changes occur) was performed. As can be seen in figure 3, the x-ray diffraction pattern of the sample treated at 400 °C displays a mixture of spectra corresponding mostly to  $\alpha$ -BaZrF<sub>6</sub> diffraction lines and incipient unknown lines. After the treatment at 600 °C, the x-ray pattern shows some remaining lines of  $\alpha$ -BaZrF<sub>6</sub> and a set of lines that could be associated with  $\beta$ -BaZrF<sub>6</sub> as reported by Parker *et al* [6]. They reported a distorted  $\beta$ -BaZrF<sub>6</sub> phase having a tetragonal cell with lattice parameters  $a = 3.85 \text{ \AA}$  and  $b = c = 5.54 \text{ \AA}$ . They have also observed that, on heating the distorted  $\beta$ -BaZrF<sub>6</sub>, the orthorhombic pattern of  $\beta$ -BaZrF<sub>6</sub> appears, concluding that the  $\beta$ -BaZrF<sub>6</sub> undergoes a lattice distortion on cooling [6]. By indexing the pattern obtained in the present work, a tetragonal cell with parameters  $a = 3.71 \text{ \AA}$  and  $b = c = 5.94 \text{ \AA}$  (close to that obtained by Parker *et al*) was found.

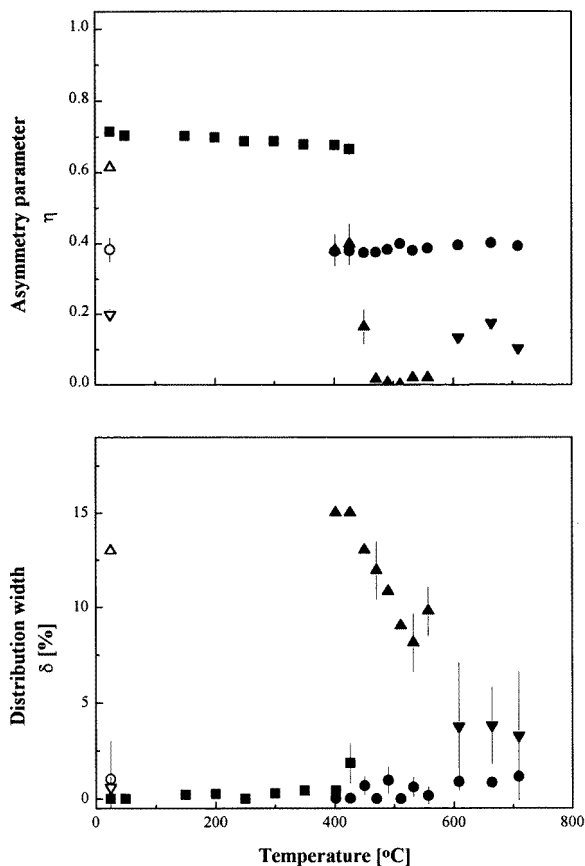
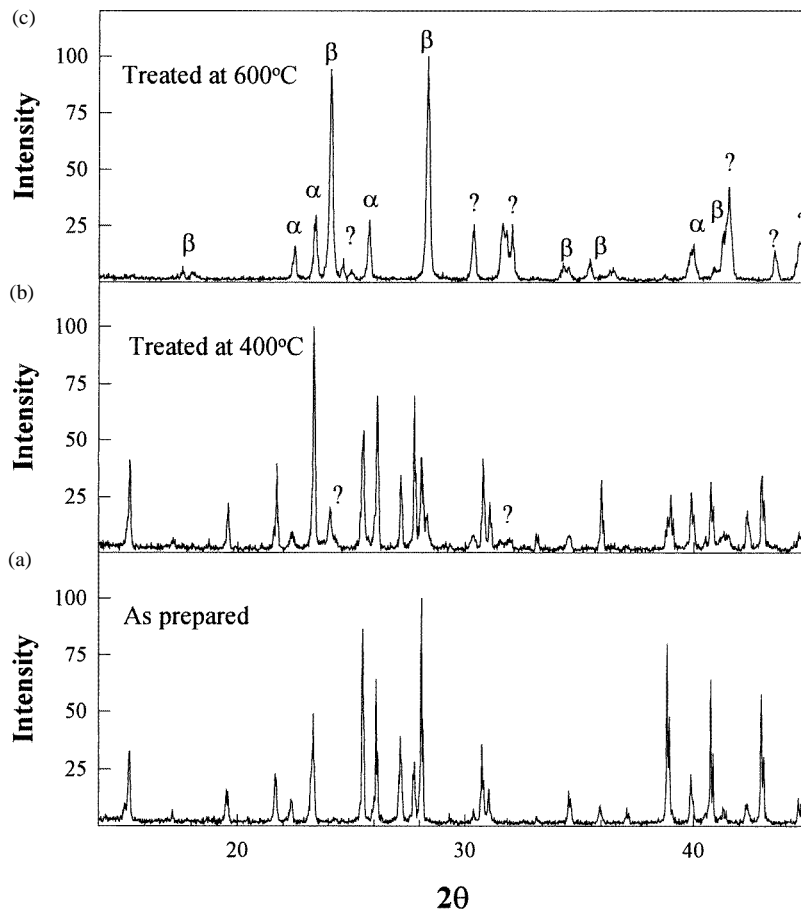


Figure 2. (Continued)

In the light of this information, PAC results at low temperatures should be interpreted as the thermal evolution of the quadrupole interaction at Zr sites in  $\alpha$ -BaZrF<sub>6</sub> ( $\omega_Q = 199.7_3$  Mrad s<sup>-1</sup>,  $\eta = 0.71_1$  at RT). The fact that only one quadrupole interaction was enough to fit the data obtained below 400 °C, clearly indicates that all Zr sites of  $\alpha$ -BaZrF<sub>6</sub> are equivalent. Unimportant changes of the hyperfine parameters occur on heating, suggesting that Zr surroundings remain nearly the same. Above 600 °C, PAC results reveal the thermal evolution of the quadrupole interaction in  $\beta$ -BaZrF<sub>6</sub> ( $\omega_Q = 113.9_2$  Mrad s<sup>-1</sup>,  $\eta = 0.40_1$  at 608 °C).

A PAC spectrum taken at room temperature after heating at 560 °C indicated the presence of the same two interactions needed to fit the spectrum at 600 °C but with interchanged populations and also a small amount of the low-frequency interaction existing at 560 °C (triangle in figure 2). Regarding the x-ray results obtained at RT after heating at 600 °C and keeping in mind that the  $\beta$ -BaZrF<sub>6</sub> phase suffers a distortion on cooling [6], it could be concluded that the most populated interaction observed at RT characterizes the zirconium sites in distorted  $\beta$ -BaZrF<sub>6</sub> and the accompanying, high-frequency interaction, characterizes the orthorhombic  $\beta$ -BaZrF<sub>6</sub>.

As shown in figure 2, the evolution of the hyperfine interaction from that associated with  $\alpha$ -BaZrF<sub>6</sub> to that associated with  $\beta$ -BaZrF<sub>6</sub> occurs within a wide temperature range (400–



**Figure 3.** (a) X-ray pattern obtained at RT in the as-prepared sample. The pattern corresponds to  $\alpha$ -BaZrF<sub>6</sub>. (b) Pattern obtained at RT after a 400 °C treatment for one day. (c) Pattern obtained at RT after a 600 °C treatment for one day. Question marks denote unidentified lines.

600 °C) and involves a third quadrupole interaction ( $\omega_Q = 47_1$  Mrad s<sup>-1</sup>,  $\eta = 0$ ) having a rather varying distribution. No compound could be associated with this interaction by x-ray analysis. Probably, this distributed interaction represents early stages of Zr surroundings during the formation of the  $\beta$ -BaZrF<sub>6</sub>.

#### 4. Conclusion

The hyperfine quadrupole parameters of  $\alpha$ -BaZrF<sub>6</sub> and  $\beta$ -BaZrF<sub>6</sub> at Zr sites have been determined. PAC results together with x-ray analysis allow us to interpret the thermal evolution of the hyperfine interaction as an extended phase transition from  $\alpha$ -BaZrF<sub>6</sub> to  $\beta$ -BaZrF<sub>6</sub>. The phase transition involves the existence of an unknown intermediate phase. It was observed that the  $\beta$ -BaZrF<sub>6</sub> compound exhibited a phase transition (orthorhombic $\leftrightarrow$ tetragonal) on cooling, with both phases clearly distinguished by PAC. Even though the experiments addressed in this paper are not directly related to a vitreous

phase of the BaF<sub>2</sub>/ZrF<sub>4</sub> system, the conclusions drawn from our experiments are of great importance in interpreting the crystallization of these kinds of fluorozirconate glass.

### Acknowledgments

One of the authors (MAT) gratefully acknowledges Dr M Ceolín for helpful discussions. The authors would like to thank Ing N H Martinez and his group for technical assistance. Partial financial support by CONICET and CICPBA is also acknowledged.

### References

- [1] Ko S-H and Doremus R H 1991 *Phys. Chem. Glasses* **32** 196
- [2] Parker J M 1989 *Ann. Rev. Mater. Sci.* **19** 21
- [3] Almeida R M and Mac Kenzie J D 1981 *J. Chem. Phys.* **74** 5958
- [4] Kawamoto Y, Horisaka T, Hirao K and Soga N 1985 *J. Chem. Phys.* **83** 2398
- [5] Laval J P, Frit B and Gaudreau B 1979 *Rev. Chim. Minèr.* **16** 509
- [6] Parker J M, Ainswoth G N, Seddon A B and Clare A 1986 *Phys. Chem. Glasses* **27** 219
- [7] Melhorn B and Hoppe R 1976 *Z. Anorg. (Allg.) Chem.* **425** 180
- [8] Laval J, Papiernik R and Frit B 1978 *Acta Crystallogr. B* **34** 1070
- [9] Steffen R M and Frauenfelder H 1964 *Perturbed Angular Correlations* ed E Karlsson, E Matthias and K Siegbahn (Amsterdam: North-Holland) p 997